AECL EACL

AECL-11718, COG-96-566-I

Corrosion of Copper Containers Prior to Saturation of a Nuclear Fuel Waste Disposal Vault

Corrosion des conteneurs en cuivre avant la saturation d'une enceinte de stockage des déchets de combustible nucléaire

Fraser King, Miroslav Kolář

December 1997 decembre

AECL EACL

CORROSION OF COPPER CONTAINERS PRIOR TO SATURATION OF A NUCLEAR FUEL WASTE DISPOSAL VAULT

by

Fraser King and Miroslav Kolář

Whiteshell Laboratories
Pinawa, Manitoba, Canada R0E 1L0
1997

AECL-11718
COG-96-566-I

AECL EACL

CORROSION OF COPPER CONTAINERS PRIOR TO SATURATION OF A NUCLEAR FUEL WASTE DISPOSAL VAULT

by

Fraser King and Miroslav Kolář

ABSTRACT

The buffer material surrounding the containers in a Canadian nuclear fuel waste disposal vault will partially desiccate as a result of the elevated temperature at the container surface. This will lead to a period of corrosion in a moist air atmosphere. Corrosion will either take the form of slow oxidation if the container surface remains dry or aqueous electrochemical corrosion if the surface is wetted by a thin liquid film. The relevant literature is reviewed, from which it is concluded that corrosion should be uniform in nature, except if the surface is wetted, in which case localized corrosion is a possibility.

A quantitative analysis of the extent and rate of uniform corrosion during the unsaturated period is presented. Two bounding cases are considered: first, the case of slow oxidation in moist air following either logarithmic or parabolic oxide-growth kinetics and, second, the case of electrochemically based corrosion occurring in a thin liquid film uninhibited by the growth of corrosion products.

Whiteshell Laboratories
Pinawa, Manitoba, Canada R0E 1L0
1997

AECL-11718
COG-96-566-I

AECL EACL

CORROSION DES CONTENEURS EN CUIVRE AVANT LA SATURATION D'UNE ENCEINTE DE STOCKAGE DES DÉCHETS DE COMBUSTIBLE NUCLÉAIRE

par

Fraser King et Miroslav Kolář

RÉSUMÉ

Le matériau tampon entourant les conteneurs dans une enceinte de stockage des déchets de combustible nucléaire canadienne se déshydratera partiellement en raison de la température élevée de la surface du conteneur. Ceci entraînera une période de corrosion dans une atmosphère d'air humide. La corrosion prendra soit la forme d'une oxydation lente si la surface du conteneur reste sèche ou d'une corrosion électrochimique aqueuse si la surface est mouillée par une fine pellicule de liquide. On étudie la documentation pertinente, à partir de laquelle on conclut que la corrosion devrait être uniforme de par sa nature, sauf si la surface est mouillée, auquel cas la corrosion localisée est possible.

On présente dans le présent document une analyse quantitative de l'ampleur et de la vitesse de la corrosion uniforme lors de la période non saturée. Deux cas limites sont pris en compte : en premier lieu, le cas de l'oxydation lente dans l'air humide à la suite de la cinétique de formation des oxydes logarithmique ou parabolique, et, en deuxième lieu, le cas de la corrosion électrochimique survenant dans une fine pellicule de liquide non inhibée par la propagation des produits de corrosion.

Laboratoires de Whiteshell
Pinawa (Manitoba) Canada R0E 1L0
1997

AECL-11718
COG-96-566-I

CONTENTS

1. INTRODUCTION

Prior to saturation with groundwater, the clay-based sealing materials surrounding the containers in a Canadian nuclear waste disposal vault are expected to become partially desiccated as a result of the movement of moisture down the temperature gradient away from the containers. As a consequence, the containers may initially undergo a period of corrosion in a warm, moist vapour phase. This period of unsaturated conditions has been assumed to be less important than the saturated period in the assessment of the corrosion behaviour of the containers (Johnson et al. 1994, 1996; Werme et al. 1992). However, the extent of corrosion during this pre-saturation period warrants investigation, since the corrosion behaviour of materials in moist atmospheres can be very different from that observed when immersed in solution.

The degree to which the buffer and backfill materials will become desiccated is not known with certainty and, in any case, will vary from container to container. In general, water will be driven away from the container due to the heat generated from the waste, but will move towards the container as a result of groundwater entering the vault from the surrounding rock. In disposal vaults located beneath the water table, as in the Canadian concept, there will be a transitory period before establishment of fully saturated conditions in the vault. In the Yucca Mountain Project, however, in which the repository will be above the water table, the vault is being designed so that the surface of the containers will be dry for a certain period of time (~1000 a) in order to delay the onset of corrosion (Gdowski and Estill 1996).

Here, we will discuss the effects of unsaturated conditions on the corrosion behaviour of copper containers in a Canadian disposal vault. The evidence for the formation of an unsaturated phase will be briefly reviewed, followed by a discussion of the likely effects on container corrosion. The impact of unsaturated buffer on the uniform corrosion of the container will then be assessed quantitatively using a simple air oxidation model and a modified version of our detailed aqueous corrosion model. These two models represent bounding calculations on the rate of uniform corrosion during the unsaturated phase.

2. MOISTURE CONTENT TRANSIENT IN VAULT

The partial desiccation of the buffer material surrounding the container has been demonstrated in both laboratory- and engineering-scale experiments (Johnson et al. 1994). Moisture is driven away from the container by the heat produced by the decay of the fuel. As the temperature gradient decreases, water flowing in the surrounding rock enters the vault and saturates the sealing materials. In general, the spatial and temporal variation of the moisture content of the buffer depends on the heat output of the container, the hydraulic conductivity of the rock and the properties of the materials in the vault

(e.g., the dependence of the hydraulic conductivity and suction potential of the buffer and backfill on moisture content, the initial moisture content of the sealing materials).

Engineering-scale tests have been performed in the Stripa project and in the buffer-container experiment (BCE) at the Underground Research Laboratory (URL). Moisture content transients in highly compacted bentonite were observed in the six tests performed at Stripa (Johnson et al. 1994). Moisture was driven away from the heaters used to simulate the containers, but collected in cooler parts of the buffer, which became saturated with water. In "wet" boreholes, i.e., in tests using boreholes that intersected water-bearing fractures, the buffer became completely saturated in as little as 1 a, whereas in "dry" boreholes, the dry zone close to the heater persisted throughout the ~3-a-period of the test (Johnson et al. 1994). A similar redistribution of the initial moisture in the buffer was observed in the BCE at the URL (Wan 1996). As at Stripa, a "halo" of saturated buffer was formed surrounding the inner dry layer. The interfacial moisture content of the buffer closest to the heater dropped to 12-13% (by dry mass), ~50% of the saturated moisture content.

The formation of a layer of saturated buffer (or backfill) surrounding a drier, inner core is an important observation in terms of the corrosion behaviour of the container. The most important characteristic of the disposal vault from the viewpoint of corrosion is that it is sealed and that the total amount of O_2 available for corrosion is limited to that trapped initially in the pores of the buffer and backfill materials. If the buffer and backfill dry out, rapid O_2 transport could occur resulting in higher corrosion rates. Then, if there is a source of O_2, additional oxidants may enter the vault. This is of particular concern during the operational phase of the vault, during which the accessways may be left open to permit monitoring and other vault operations. Then, the presence of atmospheric air represents a significant source of additional O_2. The experimental observations suggest, however, that it is unlikely that the buffer and backfill will desiccate as far as the bulkheads sealing the rooms, so that the rooms will remain effectively sealed against O_2 ingress.

Various attempts have been made to predict the extent of the moisture content transient in a disposal vault. These predictions, however, are severely restricted by the variability of the rock properties from site to site and, even, within a given disposal room. Nevertheless, Johnson et al. (1994) estimated that, for rock of low hydraulic conductivity ($<10^{-13}$ m·s^{-1}), it could take thousands of years for the vault to saturate. Thomas and Onofrei (1996) used a coupled thermo/hydro/mechanical model to predict the resaturation time of an in-room configuration disposal vault. For rock with a hydraulic conductivity of 10^{-10} m·s^{-1} (used to simulate a permeable geosphere, Johnson et al. (1996)), resaturation occurred in as little as 12 a (Thomas and Onofrei 1996). However, the uncertainty in the predictions was large because of the uncertainty in the properties of the buffer and backfill materials. Varying the value of the coefficient of specific moisture capacity of the light backfill, alone, resulted in resaturation times of 14 to >250 a.

In conclusion, therefore, the experimental data indicate that partial desiccation of the sealing materials will occur, but the results of the modelling studies suggest that its extent will be very difficult to predict. However, it seems likely that the vault will be effectively sealed at all times, so that no additional O_2, over and above that trapped in the pores of the buffer and backfill, should enter the vault.

3. EFFECT OF UNSATURATED CONDITIONS ON CONTAINER CORROSION

Given that the buffer will dry out, there will be a period during which the container will be exposed to a moist atmosphere. There are, then, two important questions that need to be addressed: (i) will the surface of the container become wet and (ii) will the container be more susceptible to localized corrosion in a moist atmosphere than under saturated conditions? If the surface does not wet, surface oxidation will occur, albeit slowly at the relatively low temperatures expected at the container surface (<100°C). If the surface does wet, aggressive conditions may form within the thin liquid film on the container surface. These two situations, and the consequences for corrosion of the container, are illustrated schematically in Figure 1.

3.1 SURFACE WETTING

Surface wetting can be viewed from both a kinetic and a thermodynamic standpoint. Kinetically, the temperature (T) gradient at the container surface will act as a driving force, causing moisture to move away from the surface and collect in cooler parts of the vault. According to this kinetic argument, liquid water will not form at the container surface until the T gradient diminishes. From a thermodynamic perspective, water will move towards regions of low water activity (a_W). There are two factors that will affect a_W on the container surface and within the buffer material. Within the buffer, a_W is determined by the suction potential that develops due to the porous nature of the material and by the osmotic potential related to the presence of salts within the pore solution. Similar forces act on the container surface; capillary forces due to the porous nature of the corrosion products and an osmotic pressure because of the concentrated solutions that form in the thin liquid film.

It is unclear which of these surfaces (the container surface or the surfaces of the buffer material) will have the lower a_W and be wetted preferentially. The magnitude of the suction potential of the reference buffer material (which inevitably also includes a component due to the osmotic potential from dissolved salt impurities in the clay) suggests that the activity of water in desiccated buffer (moisture content of 14% at 20°C, ~60% of the saturated moisture content) could be as low as 0.95 (King 1996a). Since the porosity of the corrosion product layer on the container is unknown, it is not possible to calculate an equivalent a_W value for the container surface as a result of capillary forces. On the other hand, the decrease in a_W due to the evaporation of a salt film on the container surface can be estimated. Concentrated solutions of hygroscopic salts, such as

$CaSO_4$ or $CaCl_2$, could form on the container surface due to evaporation. The water activity of an 8 $mol \cdot kg^{-1}$ solution of $CaCl_2$ is ~0.26 (Robinson and Stokes 1959).

Because of the uncertainty over whether water will condense on the surface of a container, two limiting cases will be examined in this report: (i) the case of a perfectly dry container surface and, (ii) the case in which the container surface is wetted by a thin liquid film.

The impacts of these two limiting cases on the corrosion behaviour of the container are quite different. For the case of the perfectly dry surface, corrosion will be limited to relatively slow oxidation in air at temperatures <100°C. Oxidation will be uniform in nature, with the rate controlling process being the diffusion of ions or electrons through the thickening oxide film. Localized corrosion is unlikely to occur, since anodic and cathodic electrochemical processes, the spatial separation of which leads to localized attack, cannot be supported in the absence of an aqueous phase. Some surface roughening may occur if the oxide is non-adherent and spalls from the surface in an uneven fashion, although the majority of studies suggest that adherent films should form.

Quite different processes will occur if the surface is wetted. Surface coverage by 15-90 water layers is believed to be sufficient to support aqueous electrochemical processes (Shreir 1976). Corrosion in moist atmospheres is often different from, and more severe than, that in bulk solution. Concentrated salt solutions can form in the small volume of water in the surface film, especially under conditions of heat transfer. Furthermore, dissolved metal ions are unable to diffuse away from the corroding surface, resulting in high interfacial concentrations and a propensity for precipitation. In addition, the supply of O_2 to the surface is faster in air than in solution. As a consequence, O_2 transport is less likely to be rate-limiting in moist air as compared with the situation in bulk solution. One possible rate-limiting factor in the vapour phase that does not generally occur in other environments, however, is the supply of H_2O.

The formation of a thin surface film may also increase the likelihood of localized corrosion. Localized corrosion is caused by a physical separation of anodic and cathodic sites, and is most severe when a small anode is coupled to a large cathode. This separation may be facilitated in thin liquid films on a surface covered by precipitated salt films and porous corrosion products (Figure 2). Occluded regions underneath deposits or in the small pores of corrosion products will tend to wet preferentially due to higher capillary and osmotic pressures. Such sites will naturally tend to become anodic sites because of spatial restrictions on the ingress of O_2. Rapid reduction of O_2 will occur on surfaces outside of these occluded regions if they are also covered by a thin liquid film. Unlike the situation in bulk solution or compacted media, the reduction of O_2 is unlikely to become transport limited in air because of the rapid rate of supply to the surface. The localized process will then be limited only by the rate of the anodic reaction.

3.2 FORMATION OF AGGRESSIVE ENVIRONMENTS

An additional effect of an unsaturated environment on the corrosion behaviour of Cu containers is the formation of aggressive environments that would not otherwise be formed in a saturated phase. Two possible ways in which the environment may be affected are as a result of vapour-phase γ-radiolysis and the impact of desiccation on microbial activity.

The γ-radiolysis of dry or moist air will produce species different from those produced by the radiolysis of bulk solution. King (1996b) has briefly reviewed the literature on the radiolysis of moist air, with particular focus on the formation of species that could induce the stress-corrosion cracking (SCC) of Cu. Although instances of NH_3, NO_2^- and organic acid formation have been reported during γ-radiolysis, it was concluded that the amounts formed would not be sufficient to induce SCC at the absorbed dose rates expected at the surface of a Cu container (~11 $Gy \cdot h^{-1}$ for a 25-mm-thick, packed-particulate Cu container with the reference 10-a-cooled fuel). Furthermore, any acidity produced by the formation of nitric or nitrous acid would be neutralized by the pH-buffering action of the clay. Given that, ultimately, the fuel to be disposed of may be much older than the age assumed for the reference calculations and that an essentially self-shielding, dual-wall container design (incorporating an inner 50-mm-thick C-steel shell for structural support (Johnson et al. 1996)) may be adopted, the probability that vapour-phase radiolysis will form aggressive environments is small.

Desiccation of the buffer will reduce the risk of microbially influenced corrosion (MIC) by limiting the extent of microbial activity (King 1996a). Micro-organisms, like all living creatures, require water for survival. Brown (1990) has listed the water tolerance for the growth of various micro-organisms in terms of a_W. Below $a_W = 0.95$, most bacteria will not grow. Most non-specialized microbes (those not especially adapted to live in low-moisture environments, such as halobacteriaceae) will not grow below $a_W = 0.90$. Consequently, it is argued (King 1996a) that desiccation of the buffer surrounding the container will result in the formation of a "sterile" zone, incapable of supporting microbial activity. (It is not clear, at this stage, to what degree desiccation will produce a sterile zone, i.e., one in which the native micro-organisms have been killed, as opposed to a microbially inactive zone). Of all the stressors to which the microbes in the buffer will be exposed (elevated T, γ-radiation, desiccation), desiccation is believed to be the most stringent (King 1996a).

3.3 REVIEW OF THE LITERATURE

3.3.1 Oxidation in Dry Air

Most studies of the oxidation of Cu in dry air or O_2 have been performed at elevated temperatures (>250°C), in order that measurable oxide thicknesses can be achieved in reasonable time periods. Oxide growth is found to obey one or more of the following rate laws (Rönnquist and Fischmeister 1960-61):

direct logarithmic	$x = a_1 \log(k_1 t + 1)$	(1)
inverse logarithmic	$1/x = a_2 \log(k_2 t + 1)$	(2)
cubic	$x^3 = k_3 t$	(3)
parabolic	$x^2 = k_4 t$	(4)
linear	$x = k_5 t$	(5)

where x is the film thickness, t is the time, and the a's and k's are constants in time but depend on T and oxygen concentration. (Here, we assume the oxide formed is continuous and uniform, so that the mass gain per unit surface area (the usual parameter measured and that usually used in Equations (1) through (5)) is proportional to x). The governing growth law will generally change as the film thickens. Gdowski and Bullen (1988) report that oxidation kinetics progress from logarithmic through cubic and parabolic rate laws with increasing thickness and/or temperature, although there are exceptions to this general rule for the oxidation of Cu (Rönnquist and Fischmeister 1960-61, Tylecote 1950-51).

Various models have been proposed to account for each of these observed kinetic laws (Rönnquist and Fischmeister 1960-61, Tylecote, 1950-51). The basis for all but the linear growth law (Equation (5)) is rate control by the diffusion of either Cu ions or electrons across the oxide film. Linear kinetics may be observed for very thin films, especially at low O_2 concentrations, (for which the rate of diffusion across the oxide exceeds the supply of O_2 to the oxide/gas interface) or for thick films which spall and become non-protective.

The composition of the oxide depends on a number of factors. Thicker films tend to consist of an inner layer of Cu_2O and an outer layer of CuO. In general, Cu_2O is observed at $T < 250^{\circ}C$, even though CuO is more thermodynamically stable (Rönnquist and Fischmeister 1960-61). Cuprous oxide also predominates at elevated T ($> 700^{\circ}C$) because of the decomposition of CuO.

The study of Cu oxidation at $T < 150^{\circ}C$ is complicated by slow oxidation kinetics and the disproportionate influence of factors such as surface finish, cold work and impurity content of the air (or oxygen atmosphere). Roy and Sircar (1981) report logarithmic oxidation kinetics in dry air at T between 75 and $100^{\circ}C$. Films up to 13-nm thick were observed in exposure periods up to 3 h. From Equation (1), a_1 was found to be independent of T and have a value of 11 nm and k_1 to have a value of 1.6 h^{-1} at $100^{\circ}C$ with an activation energy of 17.6 $kJ \cdot mol^{-1}$. In an earlier study, Krishnamoorthy and Sircar (1969) reported that k_1 was weakly dependent on the partial pressure of O_2 (p), $k_1 \propto p^{0.3}$.

In contrast, Pinnel et al. (1979) observed parabolic kinetics (Equation (4)) following the growth of a 1-nm-thick air-formed layer. These authors studied film growth at T between 50 and $150^{\circ}C$ for periods up to 1000 h and observed maximum film thicknesses of ~200 nm. The air used had a relative humidity (RH) of 50% at room temperature, which corresponds to an RH of between 13% and 2% at the experimental T. Thus, condensation of water on the coupon surfaces would have been avoided. At $100^{\circ}C$, $k_4 = 0.14$ $nm^2 \cdot h^{-1}$

with an activation energy of 167 $kJ \cdot mol^{-1}$. Pollutants in laboratory air were found to increase the oxidation rate by a factor of between 3 and 8 (Pinnel et al. 1979).

The results of earlier studies have been reviewed by Rönnquist and Fischmeister (1960-61) and Tylecote (1950-51).

3.3.2 Corrosion in Moist Air

The corrosion of Cu in moist air has been extensively studied. The corrosion (patination) of roofs and outdoor structures (Corrosion Science 1987, Mattsson 1982) and the corrosion of electronic devices (Lobnig et al. 1993) are two obvious areas of interest. The type of corrosion described in this section occurs when the surface is wetted by a thin film of water. Water condenses on the surface above a certain critical RH, the value of which depends on the porosity of the surface deposits and the presence of hygroscopic salts, but is typically in the range 50-70% RH (Shreir 1976). Corrosion then proceeds via electrochemical processes similar to those normally considered in aqueous solution.

Concentrated solutions can form because of the limited solution volume. The mass of water on the surface at the critical RH has been estimated to be 0.01 $g \cdot m^2$ (Mattsson 1982), equivalent to a layer thickness of 10 nm. For a typical corrosion rate of 1 $\mu m \cdot a^{-1}$ (ASM International 1987), the rate of accumulation of corrosion products would be 30 $mol \cdot dm^{-3} \cdot d^{-1}$ (Mattsson 1982). Therefore, even though the film thickness at 100% RH is estimated to be a factor of 100 larger (Mattsson 1982), corrosion in moist atmospheres is characterized by the formation of concentrated aqueous solutions.

Corrosion rates of Cu in moist atmospheres have been measured by various workers. In rural, urban and marine environments, the rates are typically ~0.5, 1-2 and ~1 $\mu m \cdot a^{-1}$, respectively (Mattsson 1982). In a series of long-term (20 a) exposure tests performed in the U.S., the mean penetration depth d (in μm) was found to be given by $d = 2.5\ t^{2/3}$, where t is the exposure time in a. The rate decreases after the first few years, indicative of a somewhat protective film. Corrosion products consist of a layer of compact Cu_2O covered by precipitated basic Cu(II) salts. The nature of the cupric species depends upon the environment, being predominantly the basic sulphate salt in rural and urban settings and the basic chloride salt in marine exposures.

Corrosion in moist air tends to be uniform in nature (ASM International 1987). Brasses containing > 15 wt.% Zn may undergo dealloying and alloys with high Mn content are prone to pitting in marine environments. Copper and brass exposed to moist atmospheres, especially rural, can be prone to SCC because of the concentrating effect of NH_3 in the thin, aerated liquid film (King 1996b).

There have been a limited number of attempts to predictively model atmospheric corrosion. Semi-empirical methods are based on the time-of-wetness and an experimentally determined mean corrosion rate, and will not be discussed further here. Mechanistic models have been developed by Graedel (1996) and King and Kolář (1995).

Graedel (1996) considers up to six zones in his model: the Gas phase, the Interface between the gas and liquid, the Liquid, the Deposition layer in which precipitation and dissolution processes occur, the Electrodic zone at which electron transfer occurs, and the bulk Solid phase. The model is known by the acronym GILDES. In concept, the GILDES model is capable of including processes such as gas-phase chemical reactions, gas-phase photolysis, absorption of gases into solution, volatilization of species into the gas phase, solution-phase chemical reactions, precipitation and dissolution of solid phases, ion transport across precipitate layers, interfacial electrochemical reactions, surface complexation reactions, etc. In practice, however, any model that includes all of these processes is computationally intractable, and for practical reasons only a limited number of these processes can be accommodated.

The GILDES model has been applied to the corrosion of Cu in atmospheres containing SO_2 (Tidblad and Graedel 1996). A total of 95 reactions were considered, including gas-partitioning, acid-base, surface-complexation, solution-complexation and various redox reactions. All processes are described kinetically, rather than by equilibrium expressions. The corroding surface was assumed to be initially covered by 1000 monolayers (ML) of Cu_2O and a 5-nm-thick layer of H_2O. Although the model was described as a corrosion model, no interfacial electrochemical reactions were included. Essentially, the model only predicts the conversion of the original Cu_2O layer to other precipitated and dissolved alteration products. As implemented, the model is capable of predicting the formation of secondary corrosion products and the time-dependent changes in the composition of the thin liquid film (of assumed constant thickness). It does not, however, predict the corrosion rate.

The GILDES model is similar in a number of ways to the numerical model developed by King and Kolář (1995). This model is also based on a kinetic description of the chemical, mass-transport, redox, adsorption/desorption, precipitation/dissolution and interfacial electrochemical processes occurring in a layered medium. To date, the model has been used to predict the corrosion rate of Cu containers in saturated and unsaturated disposal vaults (King and Kolář 1995, 1996a), the evolution of redox conditions within a disposal vault (Kolář and King 1996) and to interpret various experimental observations and natural analogue studies (King and Kolář 1996b). Under unsaturated conditions (King and Kolář 1995), the model is capable of predicting the effect of rapid O_2 diffusion through unsaturated buffer material on the corrosion rate of Cu containers. Since the thin liquid film is not explicitly modelled, however, no information is obtained about the changes in composition of this layer. This model will be used below to quantitatively predict the extent of corrosion of containers covered by a thin liquid film.

3.3.3 Corrosion in Air in the Presence of γ-radiation

A number of experimental studies have been performed on the corrosion of Cu in moist and dry air subject to γ-irradiation. A difficulty in interpreting the results of these studies is knowing whether or not the specimen surfaces were wetted. Although the RH is often reported, the critical RH (CRH), above which a thin liquid film is present on the surface,

is not. Since the CRH will change in an unpredictable fashion during the course of the experiment due to the formation of hygroscopic deposits and porous corrosion products, the onset of wetting cannot be reliably predicted from the CRH in similar, unirradiated environments.

Yunker (1990) and Yunker and Glass (1987) report the results of tests in which the vapour phase was trace heated in order to maintain it at a temperature above the dew point (and, hence, avoid condensation on the specimens). Samples of Cu (UNS C10100), 7%Al-bronze (UNS C61300) and 70-30 Cu-Ni (UNS C71500) were exposed to (i) J-13 water (18 $\mu g \cdot g^{-1}$ SO_4^{2-}, 125 $\mu g \cdot g^{-1}$ HCO_3^-, 9.6 $\mu g \cdot g^{-1}$ NO_3^-, 6.9 $\mu g \cdot g^{-1}$ Cl^-) at 95°C, (ii) the vapour phase above this solution, and (iii) air/H_2O vapour at 150°C (in the latter two cases, the temperature of the vapour phase will have been several °C higher than that stated, to avoid condensation). The specimens were irradiated at an absorbed dose rate of 1000 $Gy \cdot h^{-1}$ for periods up to 16 months. The mass gain followed approximately parabolic kinetics for all three materials up to 14 months (Yunker and Glass 1987), although linear kinetics were reported for pure Cu in the vapour phase at 95°C after 16 months (Yunker 1990). For Cu, the mean uniform corrosion rate after 14 months in solution at 95°C was 2.0 $\mu m \cdot a^{-1}$, compared with 4.1 $\mu m \cdot a^{-1}$ and 0.46 $\mu m \cdot a^{-1}$ in the vapour phase at temperatures of 95°C and 150°C, respectively. The coupons were oxide covered, Cu_2O dominating at 150°C, a Cu_2O/CuO layer in the vapour phase at 95°C and CuO in the solution at 95°C. Corrosion was primarily uniform for Cu, but some pitting and crevice corrosion was noted. No SCC was observed and no NH_3 was found in the vapour phase. Although the tests were designed to simulate, and were discussed in terms of, dry-surface oxidation in irradiated air, some condensation must have occurred to support the aqueous electrochemical reactions responsible for the localized corrosion. No comparative unirradiated data were given.

Reed et al. (1990) and Reed and Van Konynenburg (1991) have also studied these three materials in irradiated air. In the first series of tests (Reed et al. 1990), samples were exposed to air/H_2O atmospheres at temperatures of 90°C, 120°C and 150°C at RH of 0%, 15% and 100% and an absorbed dose rate of 700 $Gy \cdot h^{-1}$. Corrosion was uniform (no rates given), although shallow pits were observed on a single specimen at 150°C/15% RH. Corrosion products comprised Cu_2O and CuO at 100% RH, but Cu_2O and basic cupric nitrate (crystal phase not identified) at 0% and 15% RH. The vapour phase contained N_2O and NO_2 (the hydrolysis of which produces HNO_3) after the tests. Again, no comparison was given to unirradiated tests performed under the same conditions. Critical RH values are generally in the range 50-70%, but condensation (leading to electrochemical interfacial processes and localized corrosion) seems to have occurred at a much lower RH in these experiments.

In the second series of tests (Reed and Van Konynenburg 1991), the same materials were exposed to (i) dry air, (ii) air/H_2O vapour at 94°C (RH 34%) and (iii) air/H_2O vapour at 152°C (RH 6%). A lower dose rate (110-210 $Gy \cdot h^{-1}$) was used. After ~75 d, the corrosion rate was higher at 152°C than at 94°C, and higher in the moist air than in dry air. No localized corrosion was reported. Both N_2O and NO_2 were observed in the

vapour phase, although basic cupric nitrate species were absent from the surfaces of the specimens (except for samples exposed to laboratory air for several days post test). Instead, the surfaces were oxide covered (both Cu_2O and CuO). The absence of localized corrosion makes it uncertain whether aqueous corrosion reactions were occurring. In comparison with their previous results, however, in which localized corrosion was observed at 15% RH, it would seem likely that the specimen surfaces were wetted in the 94°C (34% RH) environment. In comparison with their previous data (Reed et al. 1991), it was suggested that nitrate phases were not observed in this later study because of the lower dose rate used. If correct, this would suggest a threshold absorbed dose rate for the formation of basic cupric nitrate corrosion products of between 200 $Gy \cdot h^{-1}$ and 700 $Gy \cdot h^{-1}$.

King and Ryan (unpublished data) have also exposed Cu (oxygen-free electronic grade, UNS C10100) to irradiated moist atmospheres. Planar and creviced U-bend samples were exposed to a H_2O-saturated vapour above a concentrated synthetic groundwater solution (SCSSS, 0.97 $mol \cdot dm^{-3}$ Cl^-) at 150°C for periods of up to 10 months at an absorbed dose rate of ~5 $Gy \cdot h^{-1}$. (Creviced U-bend samples comprise two U-bend samples sandwiching a polymeric spacer material, and are designed to simultaneously test for crevice corrosion and SCC). Visual inspection of the coupons showed them to be covered by a green patina (assumed to be atacamite, $CuCl_2 \cdot 3Cu(OH)_2$). Corrosion appeared to be uniform in nature, with no extensive crevice corrosion or any indications of SCC. The coupons had clearly been wetted during the tests.

Alexandrov et al. (1987) report the results of irradiation studies of Cu and a number of other structural metals in moist atmospheres. Samples were exposed to moist air of 50-70% RH at 37°C and an absorbed dose rate of 6500 $Gy \cdot h^{-1}$ (total dose up to 2 MGy). The uniform corrosion rate was 3.0 $\mu m \cdot a^{-1}$, approximately 100 times that under unirradiated conditions. No localized corrosion was reported. The surfaces of the samples were covered by nitrates species. In separate experiments, no effect of RH (0% and 98%) on the corrosion rate of Cu was observed. As a consequence of this latter observation, and based on arguments on the effects of various air/H_2O radiolysis products, it was concluded that corrosion was caused by oxidation, rather than by aqueous electrochemical processes. Radiolytic NO_2 species were believed to accelerate corrosion and account for the surface nitrating.

The possibility of SCC of Cu due to NH_3 or NO_2^- produced by the radiolysis of moist air has been discussed by King (1996b). Neither Yunker (1990) nor King and Ryan (unpublished data) observed SCC of stressed Cu specimens at absorbed dose rates up to 1000 $Gy \cdot h^{-1}$ or T up to 150°C. However, Makepeace (1974) reports the SCC of 70-30 Cu-Zn upon irradiation in moist air (100% RH) at ambient temperature. Cracking was observed at absorbed dose rates of 5.9 x 10^4 $Gy \cdot h^{-1}$ and 1500 $Gy \cdot h^{-1}$, but in the latter case only when the moist air was contaminated by amines formed from a neoprene rubber filter. In the high-dose-rate test, corrosion products consisted of $Cu_2(OH)_3NO_3$ and $Zn(OH)_2NO_3$, with $CuCl_2 \cdot 3Cu(OH)_2$ present near the cracks. Cracking was assumed to result from NH_3 formation (Makepeace 1974), although radiolytically produced NO_2^-

could also have been responsible (King 1996b). It appears, however, that high dose rates (perhaps $>10^4$ Gy·h^{-1}) are required to induce SCC.

4. QUANTITATIVE ASSESSMENT OF THE EFFECT OF UNSATURATED CONDITIONS ON THE UNIFORM CORROSION OF COPPER

4.1 MODELS

4.1.1 Oxidation in Dry Air

Of the various kinetic expressions proposed in the literature for the oxidation of Cu in dry air, we shall use the logarithmic rate law of Roy and Sircar (1981) and the parabolic model of Pinnel et al. (1979). Both of these studies were performed at relatively low temperature (<150°C) in dry air (no surface wetting). From Equation (1), the oxide growth rate is given by

$$\frac{dx}{dt} = \frac{a_1 k_1}{2.3} \cdot \frac{1}{k_1 t + 1} \tag{6}$$

for logarithmic growth and

$$\frac{dx}{dt} = \sqrt{\frac{k_4}{4t}} \tag{7}$$

for parabolic growth. The values for the various rate constants are given in Section 3.3.1. The temperature dependence of k_1 and k_4 follows an Arrhenius relationship

$$k = k^{\circ} \exp\left(-\frac{\Delta E}{RT}\right) \tag{8}$$

where the pre-exponential factor (k°) and activation energy (ΔE) have values of 475 h^{-1} and 17.6 kJ·mol^{-1} for the logarithmic expression of Roy and Sircar (1981) and 3.5×10^{22} nm^2·h^{-1} and 167 kJ·mol^{-1} for the parabolic rate law of Pinnel et al. (1979) determined in pollutant-free standard air.

The time dependence of the surface temperature of a Cu container for the in-room emplacement configuration has been determined by Baumgartner et al. (1995) (Figure 3). This temperature profile was calculated using a constant thermal conductivity for each of the sealing materials, corresponding to that of the as-emplaced material. Since the thermal conductivity of buffer and backfill material decreases with decreasing moisture content, the container surface temperatures will be higher in partially desiccated vaults.

However, in the absence of detailed thermal predictions for unsaturated buffer, the T profile in Figure 3 will be used for the present calculations.

4.1.2 Corrosion in a Thin Liquid Film

An early version of the detailed numerical Cu container failure model will be used to determine the extent of corrosion during the unsaturated phase for the case of a thin liquid film (King and Kolář 1995). This version of the model is capable of simulating the effect of rapid O_2 transport on the vapour-phase corrosion of Cu, but not the effect of the formation of high salt concentrations in the thin liquid film. The mechanistic basis for this version of the model is illustrated schematically in Figure 4. Only two mass-transport barriers are considered in this version of the model, a 1-m-thick layer of compacted buffer material and a 50-m-thick layer of rock (King and Kolář 1995). This version of the model differs in a number of minor respects from that used for the assessment of in-room emplacement of Cu containers (Johnson et al. 1996). The most notable differences are the inclusion of four mass-transport layers in the later version, minor differences in the reaction mechanism and boundary conditions, and the assumption of isothermal conditions in the version of the model used here. None of these differences should alter the basic conclusions of the present study, however.

There are a number of assumptions made in the calculations (King and Kolář 1995). As stated above, the temperature is assumed to be constant in space and time (only the results of simulations at 25°C are given here). In addition, the moisture content of the buffer is assumed to be constant in space and time, at either 80% or 100% of the saturated moisture content. In the case of 80% saturation, the Cu surface is assumed to be covered by a sufficiently thick layer of H_2O that electrochemical reactions are possible and the supply of H_2O is not rate-limiting. Although precipitation of both Cu_2O and $CuCl_2 \cdot 3Cu(OH)_2$ is included in the model, it is assumed that precipitation of these species on the corroding surface does not inhibit the rate of corrosion. The rock layer is assumed to be saturated at all times. The chloride concentration of the surface film, and of the bulk pore fluids in the saturated case, is assumed to be 1 $mol \cdot dm^{-3}$. Electrolyte concentration processes in the thin liquid film are not simulated.

Oxygen is present in both the aqueous and vapour phases, with the concentrations in the two phases assumed to be at equilibrium and determined by Henry's law. The quantity of O_2 trapped in the pores of the buffer material initially is constant, and equivalent to that in buffer material with the reference emplacement moisture content of 80%. Consequently, for a moisture content of 100%, the initial dissolved $[O_2]$ is artificially increased in order to conserve the total amount of trapped O_2.

The effective diffusion coefficient of O_2 through the buffer (D_{EFF}) is assumed to be given by

$$D_{EFF} = \tau_S \varepsilon_{ES} D_0^S + \kappa_{EQ} \tau_V (1-S)^3 \varepsilon_{EV} D_0^V \qquad (9)$$

where τ_S and τ_V are the solution- and vapour-phase tortuosity factors, ε_{ES} and ε_{EV} are the solution- and vapour-phase effective porosities, D_0^S and D_0^V are the diffusion coefficients of O_2 in solution and vapour and κ_{EQ} relates the vapour-phase O_2 concentration (c_O^V) to the solution concentration (c_O^S) by $c_O^V = \kappa_{EQ} c_O^S$. Finally, there is assumed to be no consumption of O_2 by Fe(II) in the buffer and no corrosion supported by the interfacial reduction of Cu(II).

The requirement that the amount of trapped O_2 be the same for both values of the moisture content results in a higher initial value of c_O^S for the 100%-saturated run. Although this is apparently an artifact of the construction of the model, it may simulate what will happen in practice if rapid saturation of the buffer causes pressurization of the vapour trapped in the buffer and an increase in the partial pressure of O_2. In any case, the consequence for the present calculations is that the rates of processes proportional to c_O^S will be higher in the case of fully saturated buffer. Such processes include the interfacial reduction of O_2, the homogeneous oxidation of Cu(I) and the diffusion of O_2. The first two processes are proportional to c_O^S. Since c_O^S is ten times higher for the 100% saturated run, the rates of these processes will also be ten times higher than for partially (80%) saturated buffer. The rate of diffusion of O_2 is proportional to both c_O^S and D_{EFF}. The effect of S on D_{EFF} (Equation (9)), however, is much greater than its effect of c_O^S. The difference in D_{EFF} between S = 0.8 and S = 1.0 is a factor of 1000, much greater than the effect of S on c_O^S (a factor of 10). Therefore, the greatest effect of S on the rate of supply of O_2 to the corroding surface is through the value of D_{EFF} rather than through its (actual or artificial) effect on c_O^S.

Details of the mathematical construction of the model, the boundary and initial conditions and the values for the various parameters are given by King and Kolář (1995).

4.2 RESULTS OF ANALYSES

4.2.1 Oxidation in Dry Air

Figure 5 shows the predicted oxide growth rate against exposure time for the two mechanisms considered here. The temperature dependencies of a_1, k_1 and k_4 are taken into account through the T profile in Figure 3. The logarithmic growth rate of Roy and Sircar (1981) gives a faster initial rate than the parabolic law of Pinnel et al. (1979). As the container surface temperature increases, however, the parabolic rate increases and exceeds the logarithmic rate after ~3 a exposure. The rate of the less-highly temperature dependent logarithmic expression decreases continuously, whereas the parabolic rate law reaches a maximum growth rate of 1.9 nm·a^{-1} after 0.7 a. After this point both rates decrease with time as the respective oxide films thicken, with the logarithmic rate decreasing with t and the parabolic rate with $t^{1/2}$.

The predicted film thicknesses are plotted as a function of time in Figure 6. When plotted as a linear function of time, the films appear to reach an effective limiting film thickness, over the timescale of interest here, of ~100 nm for logarithmic growth and ~140 nm for

parabolic kinetics. (Theoretically, the films continue to thicken with time, but the film growth rates become extremely small). These film thicknesses are attained after ~50 000 a. A limiting film thickness of 140 nm would correspond to a wall penetration of 84 nm for a Cu_2O film and 80 nm for a CuO film. The amount of O_2 consumed would correspond to 2.9 x 10^{-7} mol·cm^{-2} and 5.6 x 10^{-7} mol·cm^{-2} for Cu_2O and CuO films, respectively, <0.1% of the total available of 6.2 x 10^{-4} mol·cm^{-2} O_2 (for the in-room emplacement configuration). Since the concentration of O_2 is not predicted to change appreciably during the exposure period, no error is incurred in not including the dependence of k_1 and k_4 in Equations (6) and (7) on $[O_2]$ in the calculations.

4.2.2 Corrosion in a Thin Liquid Film

The predicted corrosion rate in the presence of a thin liquid film in 80% saturated buffer material (S = 0.8) is shown in Figure 7, along with the rate predicted for fully saturated buffer (S = 1.0) for comparison. A constant temperature of 25°C was used for these simulations, as opposed to the time-dependent T profile used for the calculation of oxidation kinetics described above. Initial corrosion rates are of the order of μm·a^{-1} in both cases, but decrease faster in saturated buffer. These initial rates are of the same order of magnitude as the initial logarithmic oxidation rate (Figure 6), although much higher than the parabolic oxidation kinetics at short times. Whereas the predicted logarithmic oxidation rate decreases rapidly with time, however, the two aqueous corrosion rates are sustained for a longer period of time. The corrosion rates are predicted to exceed 0.1 μm·a^{-1} for 8.5 a and 2.4 a for S = 0.8 and 1.0, respectively, compared with a period of only 0.05 a for logarithmic oxidation kinetics.

The aqueous corrosion rate in saturated buffer clearly shows a $t^{-1/2}$ dependence, whereas that in unsaturated buffer decreases more slowly with time. Although the corrosion rate in saturated buffer is presumably diffusion limited, the nature of the rate-controlling process in unsaturated buffer is uncertain (see below). Regardless, the rate in unsaturated buffer is higher than that at S = 1.0 for the first 11 a exposure, after which the rate in unsaturated buffer material drops precipitously, being <1 nm·a^{-1} after 26 a. The precipitous decrease in corrosion rate is due to exhaustion of all of the O_2 trapped in the vault. A similar phenomenon is predicted to occur in saturated buffer, but only after ~450 a (for an equivalent corrosion rate of 1 nm·a^{-1}). One of the effects of unsaturated conditions, therefore, is a higher corrosion rate but a shorter period to consume the trapped O_2.

Figure 8 shows the predicted depth of corrosion for these two simulations as a function of time. In both cases, the maximum depth of corrosion is ~5 μm, equivalent to the extent of corrosion caused by the interfacial reduction of ~50% of the initially trapped O_2. The remaining 50% of the O_2 is consumed in the oxidation of Cu(I) to Cu(II) (denoted by rate constant k_7 in Figure 4). The major effect of unsaturated conditions, however, is to consume all the available O_2 in a shorter period, approximately 40 a compared with a period of 750 a in saturated buffer.

The maximum depth of corrosion in saturated buffer is predicted to be slightly smaller than for S = 0.8 (Figure 8). This difference is a consequence of the impact of the kinetics of the reduction of Cu(II) by Fe(II) (k_8 in Figure 4). In saturated buffer, a fraction of the Cu(II) formed by the oxidation of Cu(I) by O_2 is reduced back to Cu(I) by reaction with Fe(II). This Cu(I) is then re-oxidized by O_2 in the buffer. Since some of the Cu(I) produced by container corrosion is effectively oxidized twice, less than 50% (in this simulation, only 48%) of the original inventory of O_2 is available to support the corrosion reaction. This effect is not observed in the case of unsaturated buffer (for which, the maximum depth of corrosion is equivalent to exactly 50% of the available O_2) because the available O_2 has been completely consumed before the redox reaction between Cu(II) and Fe(II) has an impact.

It is difficult to determine which of the many processes included in the model (Figure 4) controls the rate of corrosion. It would be of interest, however, to not only identify the rate-determining step (rds), but also to determine whether it changes as the moisture content of the buffer changes. The major impact of decreasing moisture content in these calculations is to increase the rate of transport of O_2 to the Cu surface, and, to a much smaller degree, decrease the rate of diffusion of dissolved Cu away from the corroding surface.

In general, the corrosion rate may be limited by either of the two interfacial reactions (the anodic dissolution of Cu and the cathodic reduction of O_2) or by the rate of transport of either of these species to or from the corroding surface. It is possible to mathematically de-couple these processes, and to calculate the maximum rate for each of the four possible rds. The maximum rate of the anodic dissolution of Cu (for $k_{-2} = 0$) is given by

$$\frac{i_a}{F} = n_a \frac{k_1 k_2}{k_{-1}} [Cl^-]_0^2 \exp\left\{\frac{F}{RT}(E_{CORR} - E_a^0)\right\} \qquad (10)$$

where i_a is the anodic current density ($A \cdot cm^{-2}$), n_a is the number of electrons transferred ($n_a = 1$), the k's are interfacial rate constants ($cm \cdot s^{-1}$) defined in Figure 4, $[Cl^-]_0$ is the interfacial chloride concentration (1.0 $mol \cdot dm^{-3}$), E_{CORR} and E_a^0 (V_{SCE}) are the corrosion potential and standard potential for the reaction $Cu + Cl^- \leftrightarrow CuCl + e^-$, respectively, and F, R and T are Faraday's constant (96487 $C \cdot mol^{-1}$), gas constant (8.314 $J \cdot K \cdot mol^{-1}$) and absolute temperature (K), respectively.

The maximum rate of the cathodic reduction of O_2 is given by

$$\frac{-i_c}{F} = n_c k_c^0 [O_2]_0 \exp\left\{\frac{-\alpha_c F}{RT}(E_{CORR} - E_c^0)\right\} \qquad (11)$$

where i_c is the cathodic current density, n_c the overall number of electrons transferred ($n_c = 4$), $[O_2]_0$ is the interfacial concentration of O_2 (taken to be equal to the bulk $[O_2]$ for

calculating the maximum rate of O_2 reduction), and α_c and E_c^0 are the cathodic transfer coefficient and standard potential for O_2 reduction, respectively.

The diffusive flux of $CuCl_2^-$ away from the corroding surface is given by

$$J_{CuCl_2^-} = \frac{n_a \sqrt{\varepsilon_{es} \tau_s D_0} [CuCl_2^-]_0}{\sqrt{\pi t}} \quad (12)$$

where ε_{es} and τ_s are the effective porosity for mass transport and tortuosity factor of the buffer, D_0 is the bulk solution diffusion coefficient ($cm^2 \cdot s^{-1}$), t the time (s) and $[CuCl_2^-]_0$ is the interfacial concentration of $CuCl_2^-$. In deriving Equation (12), it is assumed that diffusion occurs in a semi-infinite medium with a constant interfacial concentration of $CuCl_2^-$. Reactions, such as the oxidation of Cu(I) to Cu(II) by O_2, the reverse reaction involving Fe(II) or the precipitation/dissolution of Cu_2O, could increase the interfacial flux of $CuCl_2^-$, but are not included in this analysis.

The diffusion of Cu(II) is not considered as a possible rds. Because the oxidation of Cu(I) to Cu(II) is assumed to be irreversible ($k_{-7} = 0$, Figure 4) and the interfacial reduction of Cu(II) is not included ($k_{10}/k_{-10} = 0$, Figure 4), the diffusion of Cu(II) away from the surface cannot influence the rate of dissolution as $CuCl_2^-$. Although $CuCl_2^-$ may be produced by the reduction of Cu(II) by Fe(II), Figure 8 shows that the impact of this reaction is small and is only significant for t > 10-100 a, i.e., it does not influence the rate of corrosion in unsaturated buffer.

Because the amount of O_2 is limited, the expression for the maximum diffusive flux of changes as O_2 is consumed. At short times, when O_2 is effectively diffusing from a semi-infinite layer, the flux is given by

$$J_{O_2} = \frac{n_c [O_2]_i \sqrt{D_{EFF}}}{\sqrt{\pi t}} \quad (13)$$

where $[O_2]_i$ is the initial O_2 concentration in the buffer and the effective diffusion coefficient of O_2 (D_{EFF}) is defined by Equation (9). Equation (13) applies up to times for which $t \leq 0.1\ell^2/D_{EFF}$, where ℓ is the length of the medium (100 cm).

For $0.1\ell^2/D_{EFF} \leq t \leq 0.3\ell^2/D_{EFF}$, the $[O_2]$ at the far boundary drops below $[O_2]_i$ and the semi-infinite expression in Equation (13) is no longer accurate. For this time period, the flux of O_2 is given by

$$J_{O_2} = \frac{n_c [O_2]_i \sqrt{D_{EFF}}}{\sqrt{\pi t}} \left\{ 1 - 2e^{\frac{-\ell^2}{D_{EFF} t}} + 2e^{\frac{-4\ell^2}{D_{EFF} t}} \right\} \quad (14)$$

For $t \geq 0.3\ell^2/D_{EFF}$, the flux is given by

$$J_{O_2} = \frac{2n_c[O_2]_i D_{EFF}}{\ell} e^{\frac{-\pi^2 D_{EFF} t}{4\ell^2}} \quad (15)$$

Each of these rate expressions (Equations (10)-(15)) is written as a flux in units of equiv·cm^{-2}·s^{-1}, and may be compared directly with the predicted corrosion rate expressed as i_{CORR}/F, where i_{CORR} is the corrosion current density (A·cm^{-2}).

The rates of the four possible rds are plotted along with the corresponding values of i_{CORR}/F for unsaturated (S = 0.8) and saturated (S = 1.0) buffer material in Figures 9 and 10, respectively. In both cases, it is clear that the maximum rates of the two interfacial processes (Equations (10) and (11)) exceed the predicted rate by at least three orders of magnitude, and cannot, therefore, be the rds. This is not a surprising conclusion, since the corrosion rate (Figure 7) displays a $t^{-1/2}$ dependence, consistent with diffusion control.

It is not clear from Figures 9 and 10, however, which of the transport steps is rate-determining. In both cases, the rate of the anodic transport step, the diffusion of $CuCl_2^-$ away from the surface, is lower than the predicted corrosion rate. This is obviously a calculation error, since the rate of the rds cannot be lower than the overall rate. In calculating the flux of $CuCl_2^-$ (Equation (12)), the interfacial $[CuCl_2^-]$ has been determined from the Nernst equation for the overall dissolution of Cu

$$Cu + 2Cl^- \leftrightarrow CuCl_2^- + e^- \quad (16)$$

namely,

$$[CuCl_2^-]_0 = [Cl^-]^2 \exp\left\{\frac{F}{RT}(E_{CORR} - E_a^{0}*)\right\} \quad (17)$$

where $E_a^{0}*$ is the standard potential for Equation (16) (-0.05 V_{SCE}). Part of the error involved in predicting the diffusive flux of $CuCl_2^-$ may arise because Equation (12) is based on a constant interfacial $[CuCl_2^-]$, whereas that used to determine the curves in Figures 9 and 10 is based on Equation (17), which varies with E_{CORR}. The variation of E_{CORR} in each simulation is equivalent to a change in $[CuCl_2^-]_0$ of up to three orders of magnitude. Equation (12) does correctly predict the time at which the corrosion rate drops to zero, however, but this may be coincidental because E_{CORR} becomes more negative as the corrosion rate drops, resulting in a decrease in the flux of $CuCl_2^-$.

Better agreement is found between the predicted rate and the calculated flux of O_2 to the container surface. Equally good agreement is observed for both saturated and unsaturated buffer. On this basis, the most likely rds in both saturated and unsaturated buffer is the diffusion of O_2 to the surface. There is no evidence that the nature of the rds changes as the rate of diffusion of O_2 increases with decreasing moisture content.

5. DISCUSSION

Although a detailed discussion of the impact of the unsaturated phase on the extent of uniform corrosion has been presented, the current analysis has failed to answer the two key questions posed earlier. First, it is not possible to predict, *a priori*, whether the container surface will wet. Substantial progress can be made in this area through coupled thermo/hydro/mechanical modelling to predict the spatial and temporal distribution of moisture within the buffer. This kind of modelling would provide information on the interfacial concentration of H_2O, expressed in terms of %RH, a_w or vapour pressure. This information alone, however, is insufficient to predict whether the container surface will wet. The prediction of a_w on the container surface is more intractable, and is only feasible through experimental measurement. Second, on the assumption that the surface is wetted by a thin liquid film at some stage, it is not currently possible to predict whether localized corrosion will occur. Although the potential for the separation of anodic and cathodic sites exists (Figure 2), the extent of localized damage can only be determined experimentally and predicted using statistical analysis of measured corrosion data.

It has been possible, however, to quantitatively assess the extent of uniform corrosion during the unsaturated phase using two bounding scenarios. In the first scenario, the container surface remains dry, and corrosion takes the form of surface oxidation in moist air. The rate of oxidation is low because of the relatively low temperatures and should be limited to a maximum wall penetration of <90 nm. In the second scenario, the surface is wetted by a thin liquid film and aqueous corrosion occurs. The rate of corrosion is higher in the absence of precipitated corrosion products and is limited, ultimately, only by the availability of O_2. For the simulation presented above, the maximum extent of corrosion is equivalent to 50% of the available O_2, which would correspond to a wall penetration of ~90 μm for the in-room disposal configuration. Thus, surface wetting may result in ~1000-fold increase in the extent of uniform corrosion during the unsaturated phase.

Regardless of the nature of the uniform corrosion process during the unsaturated phase, our existing predictions of the lifetimes of Cu containers remain valid. The total amount of corrosion before and after saturation of the vault is limited by the amount of O_2 trapped initially in the pores of the buffer and backfill materials. There is no evidence that partial desiccation of the buffer will permit additional O_2 to enter the vault during the operational phase. Instead, redistribution of the initial moisture in the buffer is likely to create a "halo" of saturated buffer around the container which will effectively seal the vault against O_2 ingress.

The nature of the corrosion processes during the unsaturated phase will affect the evolution of redox conditions within the vault. Kolář and King (1996) have predicted that the O_2 in a fully saturated disposal vault at a uniform temperature of 75°C would be consumed in a period of 670 a. The majority of the O_2 (60%) is predicted to be consumed by reaction with Fe(II) in the backfill material, a process not modelled here, with only 21% and 18% consumed by the interfacial reduction reaction and the homogeneous

oxidation of $CuCl_2^-$, respectively. A similar period (750 a) is predicted here for a saturated vault (S = 1.0), despite using a different set of reactions and a modified vault geometry. In contrast, the O_2 is predicted to be consumed in only 38 a in an unsaturated vault (S = 0.8). These latter two periods are equivalent to the times at which the corrosion rates decreases precipitously in Figure 7. However, if the surface of the containers remain dry, very little of the trapped O_2 will be consumed. The maximum wall penetration of ~90 nm is equivalent to <0.1% of the trapped O_2. Therefore, O_2 will only be consumed by reaction with Fe(II) minerals in regions of the vault that remain wet. As a consequence, it is likely that the majority of the O_2 will be consumed in the backfill, a process that will be limited by the slower temperature rise in the backfill and the need for the O_2 in the buffer to diffuse into the backfill in order to be consumed. It is likely, therefore, that an extended period of surface oxidation, as opposed to aqueous corrosion, will delay the establishment of anoxic conditions within the vault.

The modified version of the aqueous corrosion model used here could be improved to more accurately predict the extent of uniform corrosion during the unsaturated phase. A significant improvement would be to take into account the spatial and temporal variation in both the moisture content and temperature. Although it would, in principal, be feasible to couple the chemical and mass-transport processes modelled here with the type of thermo/hydro/mechanical model of Thomas and Onofrei (1996), the computations required would make such a complicated model impractical. Alternatively, an analytical expression for the dependence of moisture content on distance and time could be developed, based on the results of thermo/hydro/mechanical modelling. Some improvement should also be made to the treatment of the distribution of O_2 between solution and vapour phases. Currently, equilibrium is assumed and the initial solution-phase $[O_2]$ modified to conserve all O_2 trapped in the vault. An alternative approach, and one that would be consistent with the kinetic treatment used for all other processes included in the model, would be to use rate constants to describe the rate of absorption and desorption of O_2 from the vapour and solution phases, respectively. Similar kinetic approaches are used for the modelling of radiolysis in mixed liquid-gas systems.

6. CONCLUSIONS

An analysis has been carried out on the effects of a period of unsaturated conditions on the corrosion of Cu containers in a Canadian disposal vault. Corrosion will either take the form of slow oxidation in moist air if the surface remains dry or faster aqueous corrosion if the surface is wetted by a thin liquid film. Based on current knowledge, it is not possible to reliably predict whether the surface will be wetted or not. Consequently, it is also impossible to predict whether localized corrosion will occur in the event of surface wetting.

Bounding calculations have been performed to predict the maximum and minimum wall penetration as a result of uniform attack. Wall penetration will range from <90 nm in the

event of oxidation to ~90 μm for thin-film corrosion. These predictions suggest that uniform attack during the unsaturated phase will neither compromise the integrity of the container nor invalidate our current container lifetime predictions.

The potential for surface wetting and subsequent localized corrosion can only be determined experimentally. On the basis of literature reports, it seems unlikely that the irradiation of moist air will lead to stress-corrosion cracking at the dose rates expected for Cu containers.

ACKNOWLEDGEMENT

The Canadian Nuclear Fuel Waste Management Program is jointly funded by AECL and Ontario Hydro through the CANDU® Owners Group.

REFERENCES

Alexandrov, A.B., V.M. Sedov, A.F. Nechaev, N.G. Petrick, N.N. Kalyazin and E.M. Filippov. 1987. Effect of gamma radiation on metal corrosion under spent fuel storage conditions. IAEA-TECDOC-418, 181-190.

ASM International. 1987. Corrosion of copper and copper alloys. In Metals Handbook, Ninth Edition, Volume 13, Corrosion. ASM International, Metals Park, OH.

Baumgartner, P., D.M. Bilinsky, C. Onofrei, Y. Ates, F. Bilsky, J.L. Crosthwaite and G.W. Kuzyk. 1995. An in-room emplacement method for a used-fuel disposal facility - preliminary design considerations. Atomic Energy of Canada Limited Technical Record, TR-665, COG-94-533.

Brown, A.D. 1990. Microbial Water Stress Physiology. John Wiley, Chichester, U.K.

Corrosion Science. 1987. Copper patina formation, special issue Corros. Sci. 27(7).

Gdowski, G.E. and D.B. Bullen. 1988. Survey of degradation modes of candidate materials for high-level radioactive-waste disposal containers. Volume 2. Oxidation and corrosion. Lawrence Livermore National Laboratory Report, UCID-21362, Vol. 2.

Gdowski, G.E. and J.C. Estill. 1996. The effect of water vapour on the corrosion of carbon steel at 65°C. Mat. Res. Soc. Symp. Proc. 412, Materials Research Society, Pittsburgh, PA, 533-538.

CANDU® is a registered trademark of Atomic Energy of Canada Limited (AECL).

Graedel, T.E. 1996. GILDES model studies of aqueous chemistry. I. Formulation and potential applications of the multi-regime model. Corros. Sci. 38, 2153-2180.

Johnson, L.H., D.M. LeNeveu, D.W. Shoesmith, D.W. Oscarson, M.N. Gray, R.J. Lemire and N.C. Garisto. 1994. The disposal of Canada's nuclear fuel waste: The vault model for postclosure assessment. Atomic Energy of Canada Limited Report, AECL-10714, COG-93-4.

Johnson, L.H., D.M. LeNeveu, F. King, D.W. Shoesmith, M. Kolář, D.W. Oscarson, S. Sunder, C. Onofrei and J.L. Crosthwaite. 1996. The disposal of Canada's nuclear fuel waste: A study of postclosure safety of in-room emplacement of used CANDU fuel in copper containers in permeable plutonic rock: Volume 2: Vault model. Atomic Energy of Canada Limited Report, AECL-11494-2, COG-96-552-2.

King, F. 1996a. Microbially influenced corrosion of copper nuclear fuel waste containers in a Canadian disposal vault. Atomic Energy of Canada Limited Report, AECL-11471, COG-94-519.

King, F. 1996b. The potential for stress corrosion cracking of copper containers in a Canadian nuclear fuel waste disposal vault. Atomic Energy of Canada Limited Report, AECL-11550, COG-96-94.

King, F. and M. Kolář. 1995. Prediction of the lifetimes of copper nuclear waste containers under restrictive mass-transport and evolving redox conditions. CORROSION/95, NACE International, Houston, TX, paper no. 425.

King, F. and M. Kolář. 1996a. A numerical model for the corrosion of copper nuclear fuel waste containers. Mat. Res. Soc. Symp. Proc. 412, Materials Research Society, Pittsburgh, PA, 555-562.

King, F and M. Kolář. 1996b. Mechanistic modelling of the corrosion behaviour of copper nuclear fuel waste containers. Proc. Int. Conf. Deep Geological Disposal of Radioactive Waste, Canadian Nuclear Society, Toronto, ON, 5-39 to 5-50. (Also published as Atomic Energy of Canada Limited Report, AECL-11644, COG-96-327).

Kolář, M. and F. King. 1996. Modelling the consumption of oxygen by container corrosion and reaction with Fe(II). Mat. Res. Soc. Symp. Proc. 412, Materials Research Society, Pittsburgh, PA, 547-554.

Krishnamoorthy, P.K. and S.C. Sircar. 1969. Influence of oxygen pressure on the oxidation kinetics of copper in dry air at room temperature. J. Electrochem. Soc. 116, 734-736.

Lobnig, R.E., R.P. Frankenthal, D.J. Siconolfi and J.D. Sinclair. 1993. The effect of submicron ammonium sulfate particles on the corrosion of copper. J. Electrochem. Soc. 140, 1902-1907.

Makepeace, C.E. 1974. Design and analysis of corrosion experiments for testing materials exposed to gamma radiation. J. Test. Evaluation 2, 202-209.

Mattsson, E. 1982. The atmospheric corrosion properties of some common structural metals - a comparative study. Mat. Perf. 21, 9-19.

Pinnel, M.R., H.G. Tompkins and D.E. Heath. 1979. Oxidation of copper in controlled clean air and standard laboratory air at 50°C and 150°C. Appl. Surf. Sci. 2, 558-577.

Reed, D.T. and R.A. Van Konynenburg. 1991. Corrosion of copper-based materials in irradiated moist air systems. Mat. Res. Soc. Symp. Proc. 212, Materials Research Society, Pittsburgh, PA, 317-325.

Reed, D.T., V. Swayambunathan, B.S. Tani and R.A. Van Konynenburg. 1990. Corrosion product identification and relative rates of corrosion of candidate metals in an irradiated air-steam environment. Mat. Res. Soc. Symp. Proc. 176, Materials Research Society, Pittsburgh, PA, 517-524.

Robinson, R.A. and R.H. Stokes. 1959. Electrolyte Solutions. Second Edition (revised). Butterworths, London.

Rönnquist, A. and H. Fischmeister. 1960-61. The oxidation of copper. A review of published data. J. Inst. Metals 89, 65-76.

Roy, S.K. and S.C. Sircar. 1981. A critical appraisal of the logarithmic rate law in thin-film formation during oxidation of copper and its alloys. Oxid. Metals 15, 9-20.

Shreir, L.L. 1976. Corrosion. Second Edition. Newnes-Butterworths, London.

Thomas, H.R. and C. Onofrei. 1996. Modelling the short-term, near field performance of an in-room emplacement configuration. Proc. Int. Conf. Deep Geological Disposal of Radioactive Waste, Canadian Nuclear Society, Toronto, ON, 5-187 to 5-196.

Tidblad, J. and T.E. Graedel. 1996. GILDES model studies of aqueous chemistry. III. Initial SO_2-induced atmospheric corrosion of copper. Corros. Sci. 38, 2201-2224.

Tylecote, R.F. 1950-51. Review of published information on the oxidation and scaling of copper and copper-base alloys. J. Inst. Metals 78, 259-300.

Wan, A.W.L. 1996. The use of thermocouple psychrometers to measure suction and moisture transients in compacted clays. Ph.D. Thesis. University of Manitoba.

Werme, L., P. Sellin and N. Kjellbert. 1992. Copper canisters for nuclear high level waste disposal. Corrosion aspects. Swedish Nuclear Fuel and Waste Management Company Technical Report, SKB-TR-92-26.

Yunker, W.H. 1990. Corrosion behavior of copper-base materials in a gamma-irradiated environment. Final report. Westinghouse Hanford Company Report, WHC-EP-0188.

Yunker, W.H. and R.S. Glass. 1987. Long-term corrosion behavior of copper-base materials in a gamma-irradiated environment. Mat. Res. Soc. Symp. Proc. 84, Materials Research Society, Pittsburgh, PA, 579-590.

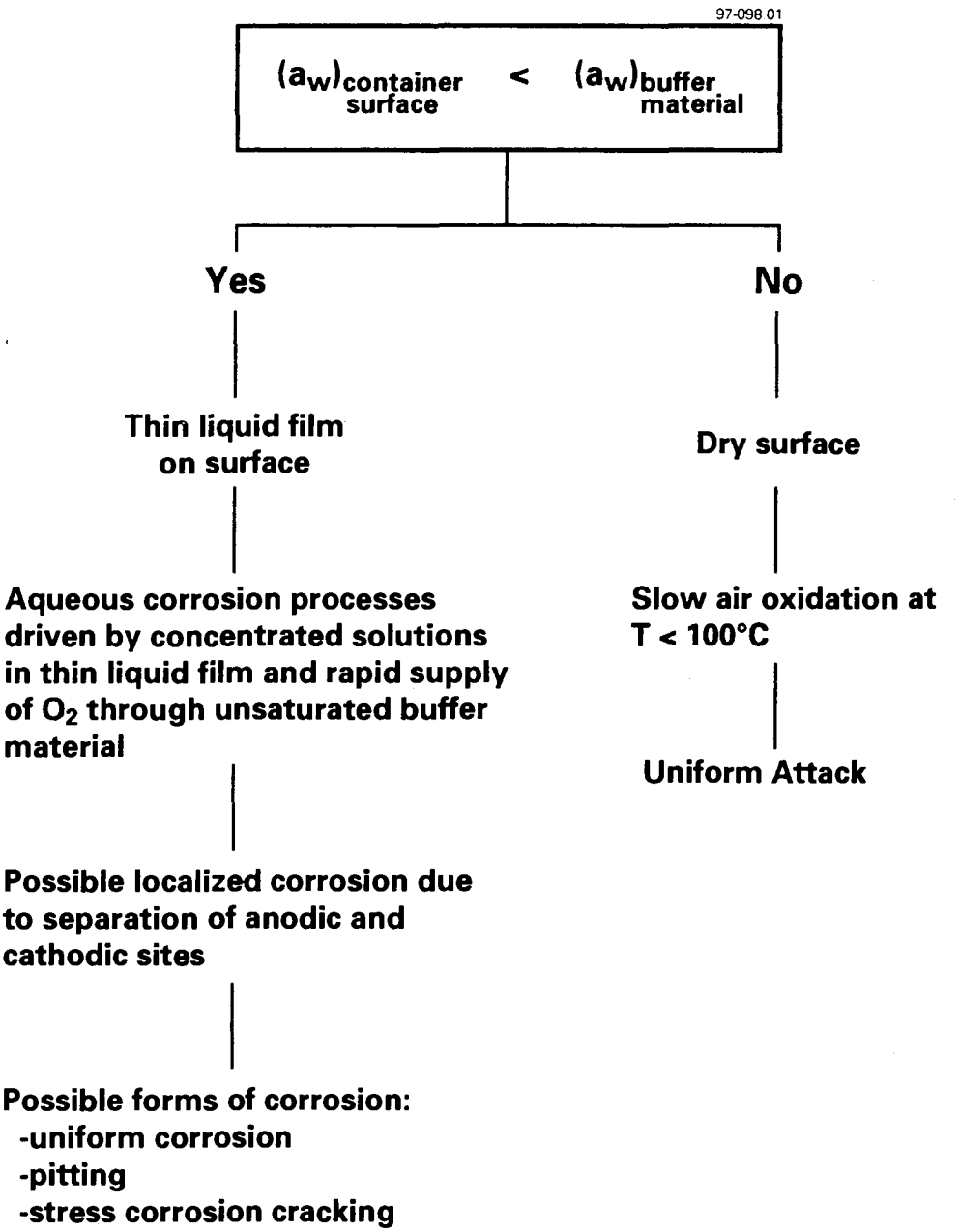

FIGURE 1: Schematic Illustrating the Corrosion Consequences of Surface Wetting

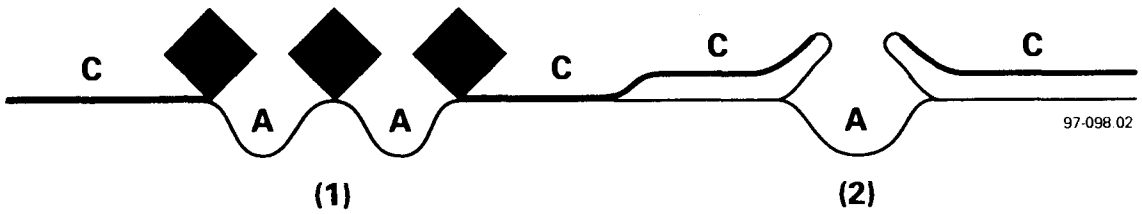

FIGURE 2: Schematic Illustrating the Possible Formation of Localized Corrosion Cells in the Event of Surface Wetting. Anodic sites (A) will tend to form in areas to which the supply of O is restricted, such as (1) underneath precipitated deposits or (2) within the pores and cracks in partially spalled corrosion products. Anodic dissolution at these sites is supported by O_2 reduction on exposed cathodic sites (C).

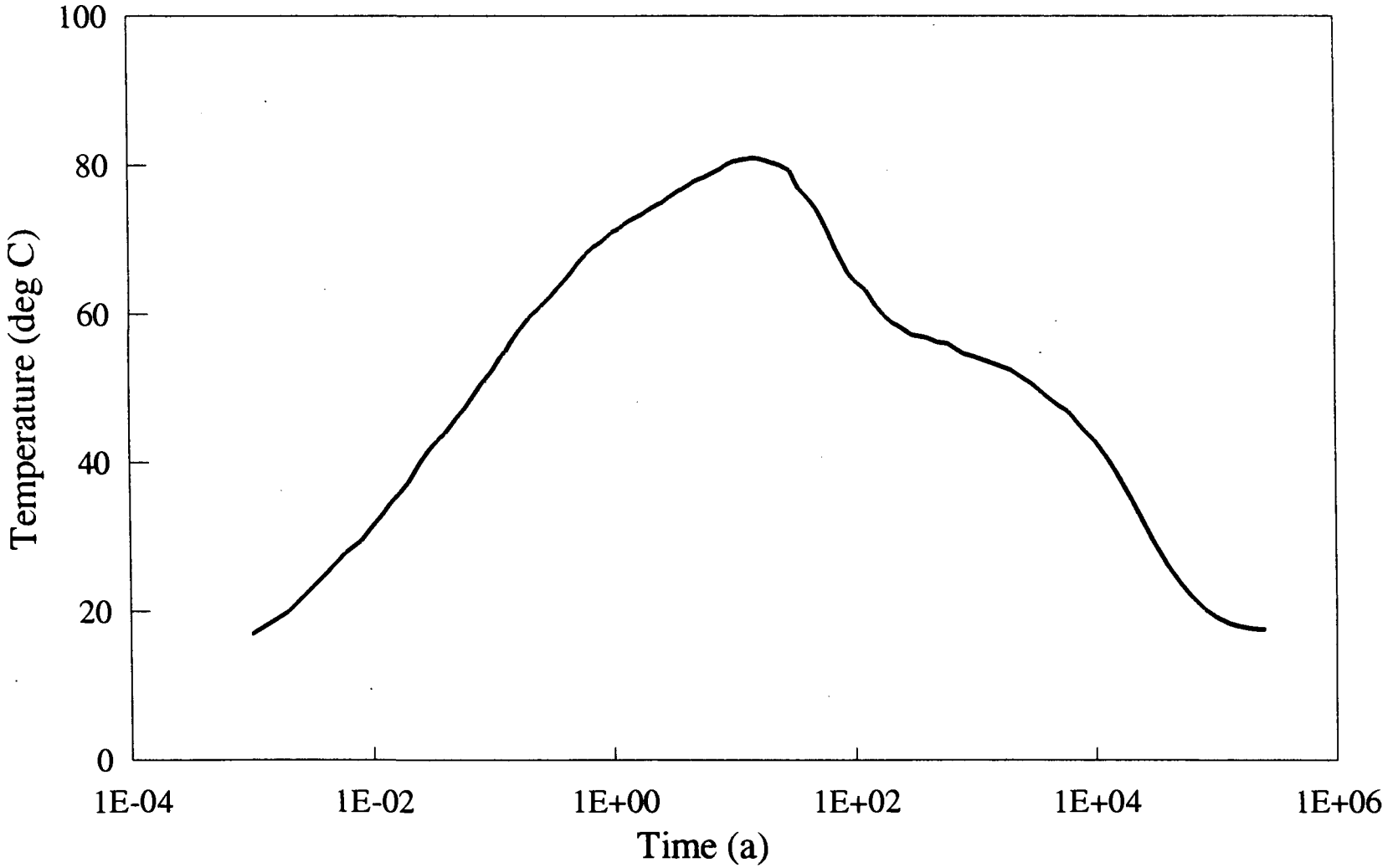

FIGURE 3: Predicted Variation of the Container Surface Temperature with Time for the In-room Disposal Configuration (Baumgartner et al. 1995)

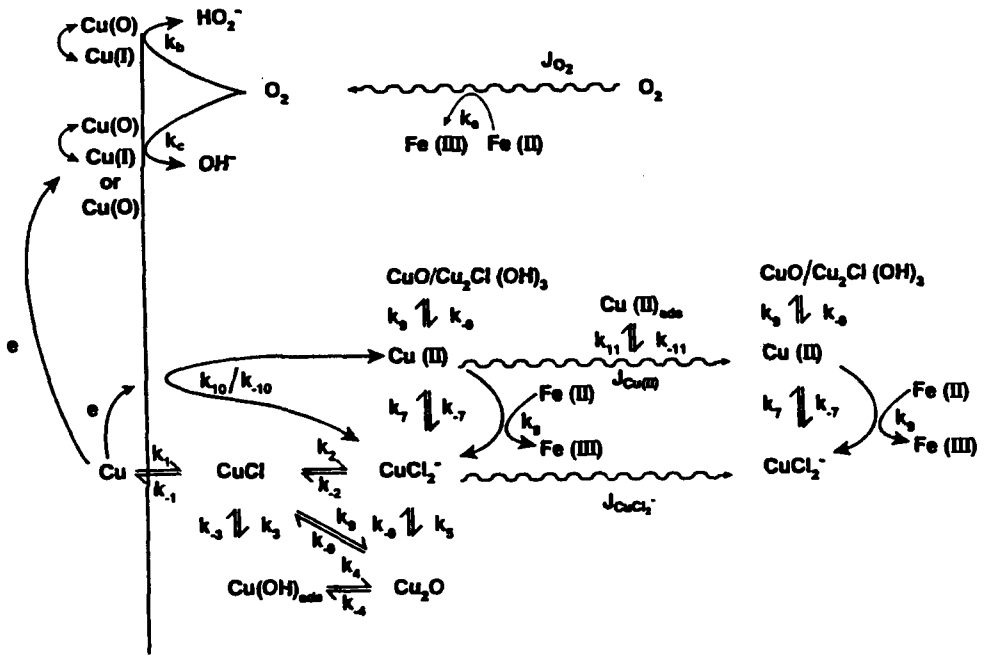

FIGURE 4: Reaction Mechanism Used to Model Aqueous Corrosion in Saturated and Unsaturated Disposal Vaults (King and Kolář 1995)

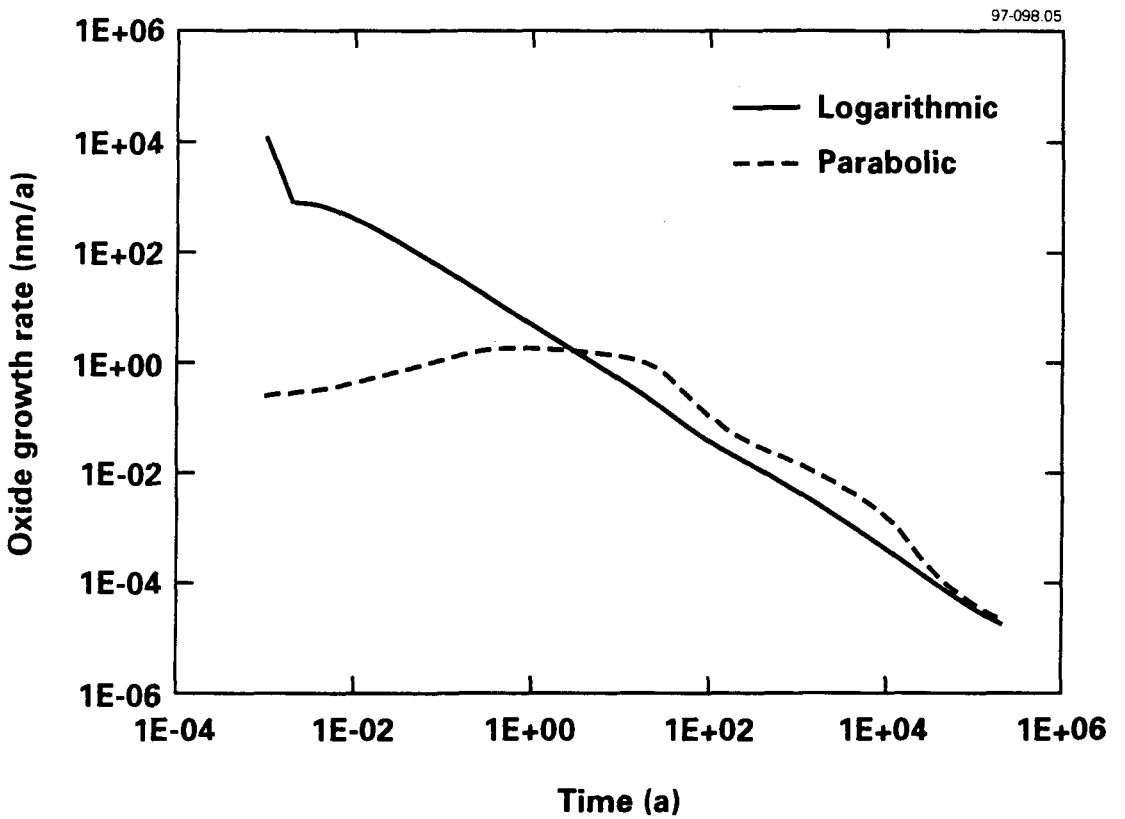

FIGURE 5: Predicted Oxide Growth Rate on Dry Container Surface for Logarithmic and Parabolic Kinetics. Logarithmic (Roy and Sircar 1981) solid curve, parabolic (Pinnel et al. 1979) broken curve.

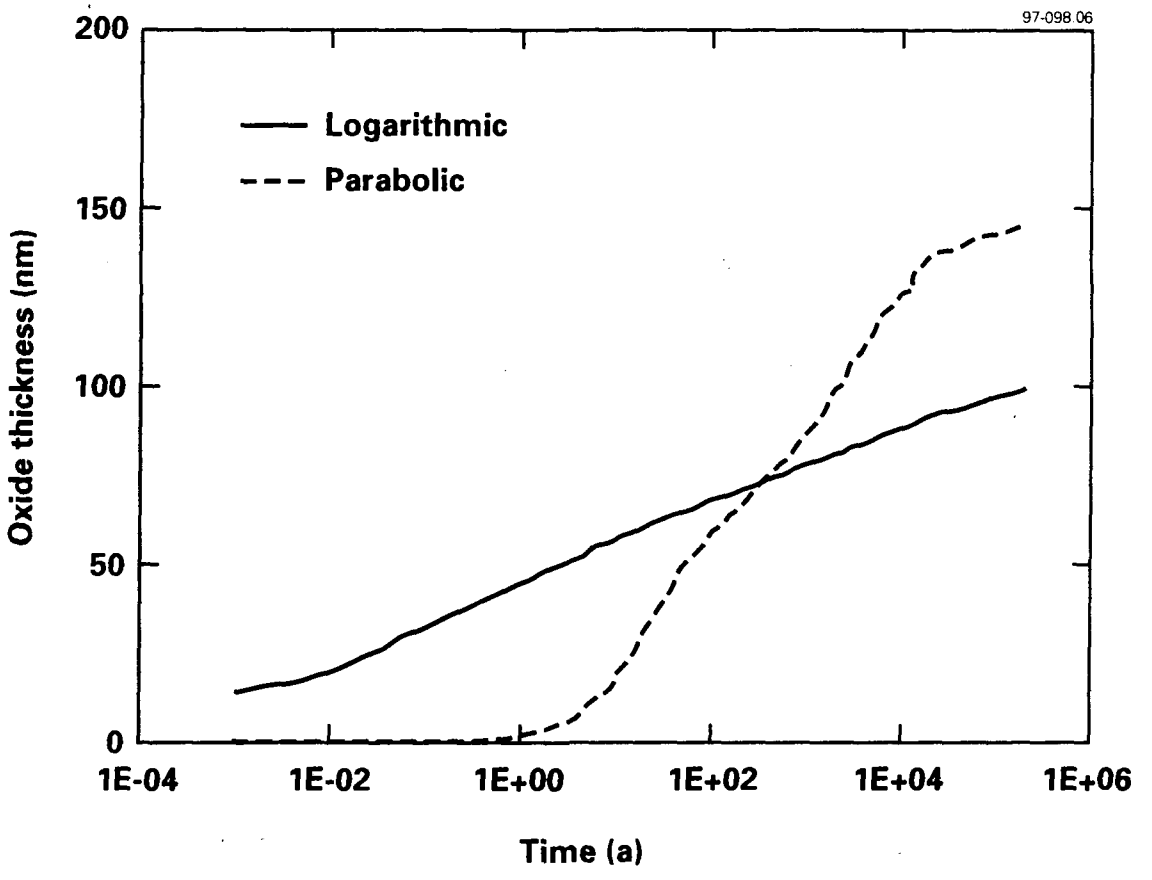

FIGURE 6: Predicted Oxide Thickness as a Function of Time for Logarithmic and Parabolic Kinetics. Logarithmic (Roy and Sircar 1981) solid curve, parabolic (Pinnel et al. 1979) broken curve.

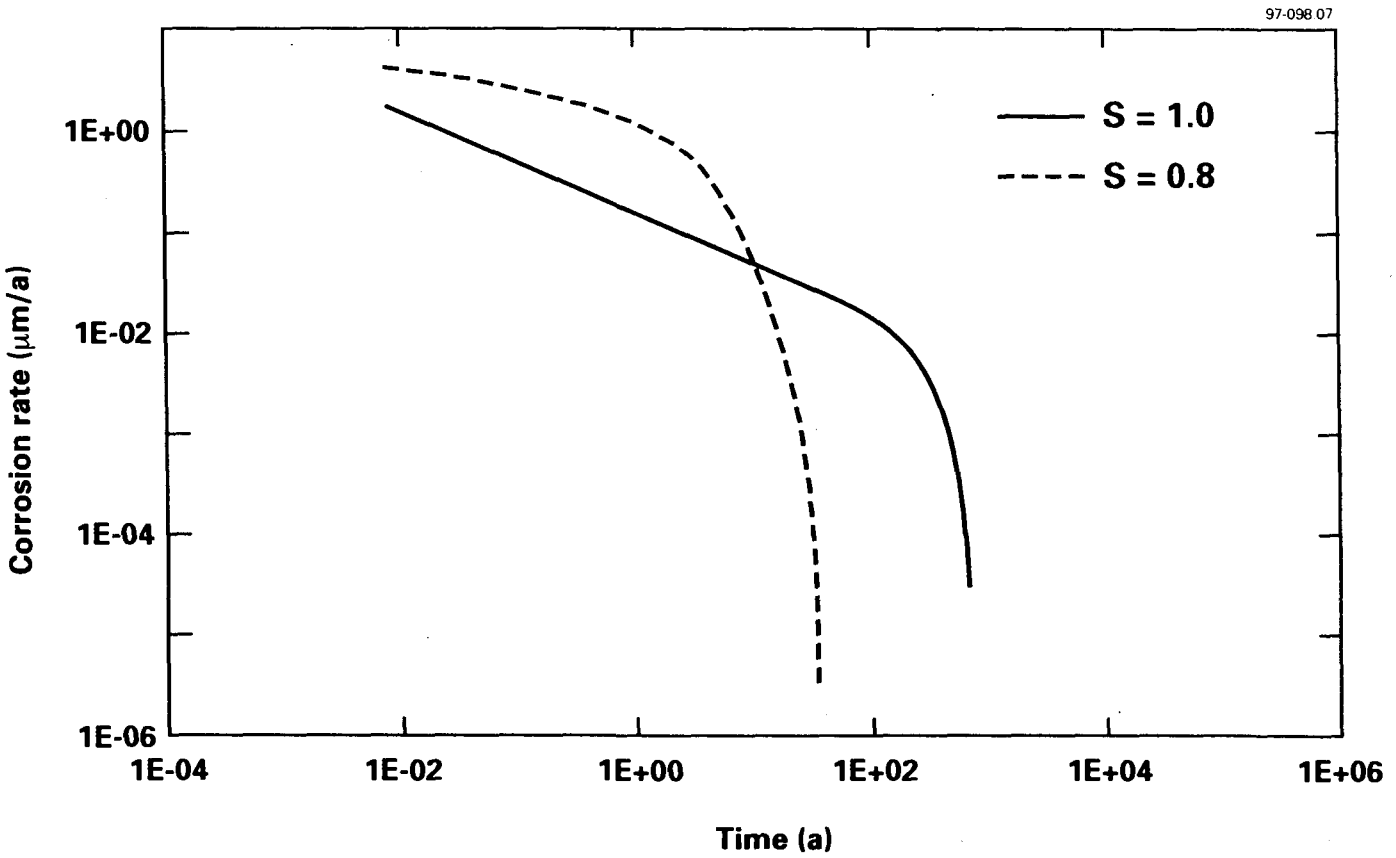

FIGURE 7: Predicted Corrosion Rate of Copper Container at 25°C in a Saturated Disposal Vault (S = 1.0) and for a Container Covered by a Thin Liquid Film (S = 0.8). Degree of saturation (S) = 0.8 (broken curve) and 1.0 (solid curve).

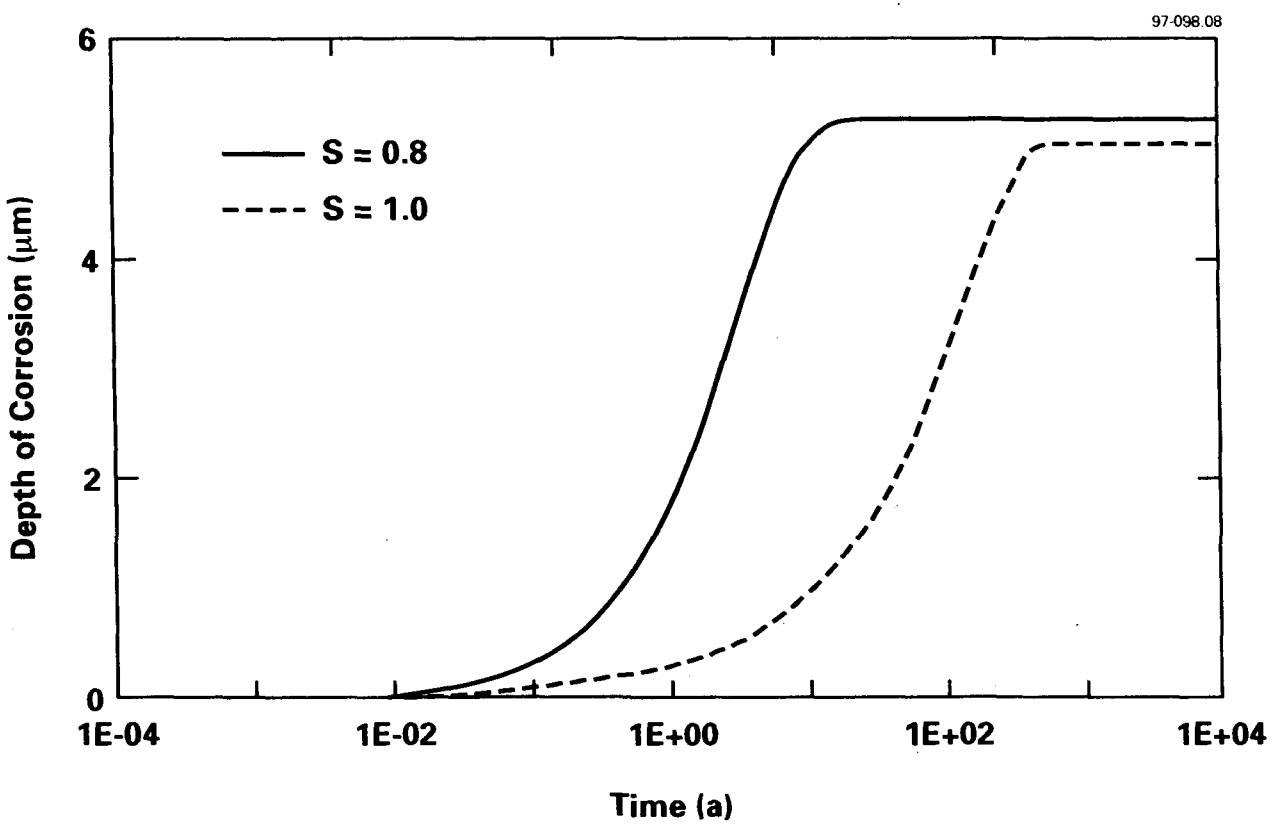

FIGURE 8: Predicted Wall Penetration as a Consequence of Aqueous Corrosion in Saturated and Partially Unsaturated Disposal Vaults. S = 0.8 (solid curve), S = 1.0 (broken curve).

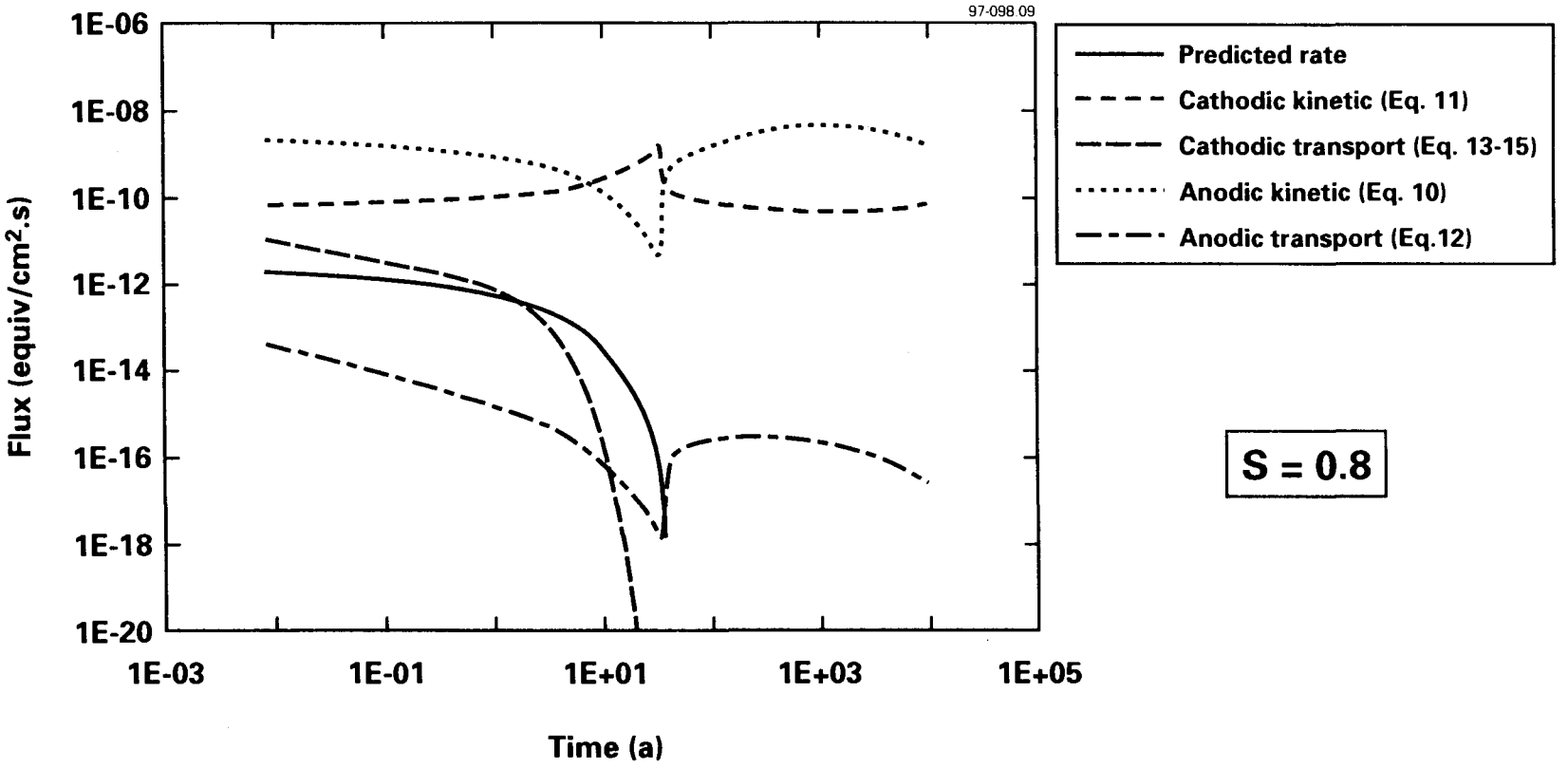

FIGURE 9: Comparison of Predicted Corrosion Rate and Rates of Four Possible Rate-determining Steps for the Uniform Corrosion of Copper Containers in an Unsaturated Disposal Vault (S = 0.8).

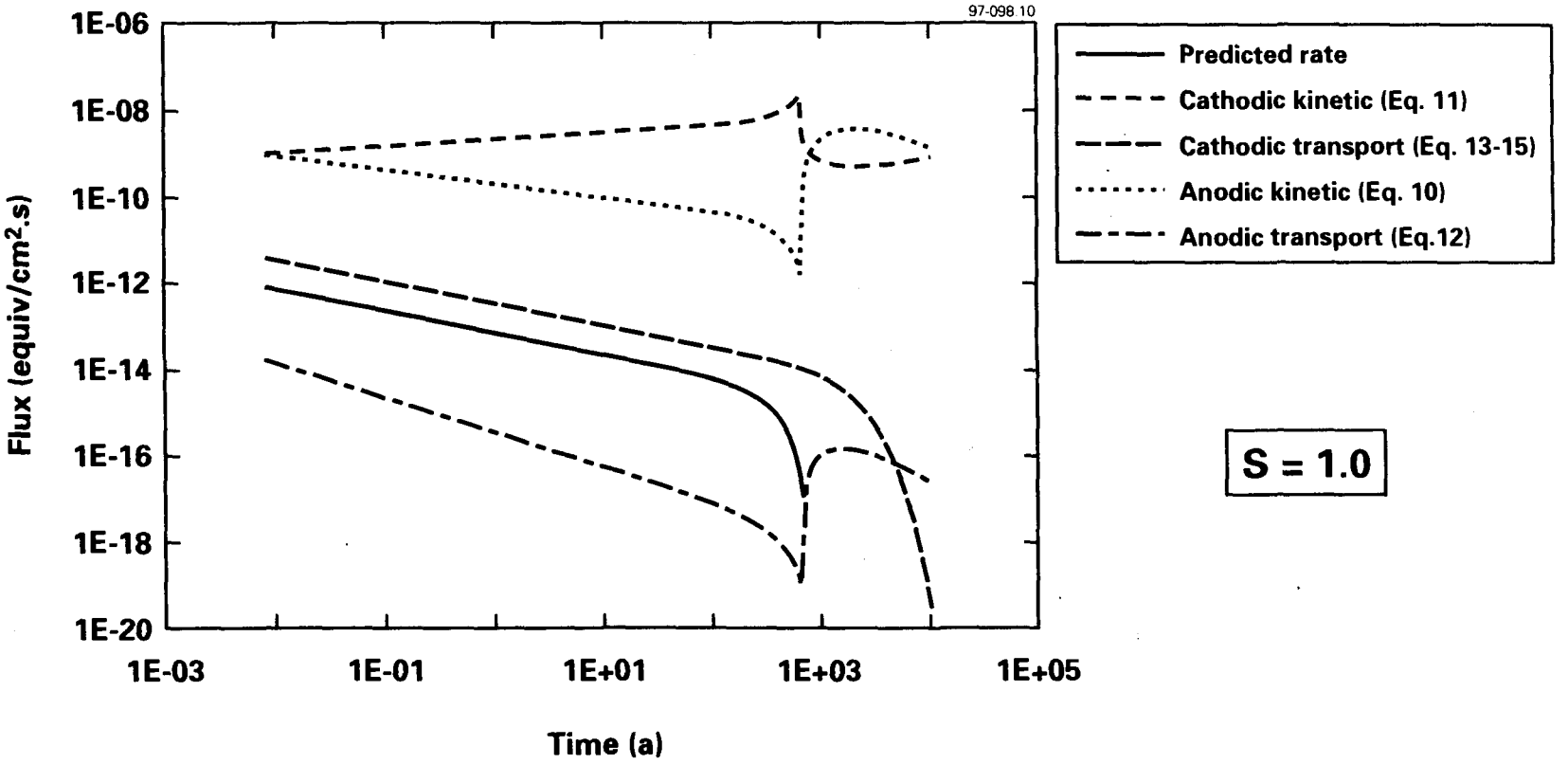

FIGURE 10: Comparison of Predicted Corrosion Rate and Rates of Four Possible Rate-determining Steps for the Uniform Corrosion of Copper Containers in a Saturated Disposal Vault (S = 1.0).

Cat. No. / Nº de cat.: CC2-11718E
ISBN 0-660-17266-6
ISSN 0067-0367

To identify individual documents in the series, we have assigned an AECL- number to each. Please refer to the AECL- number when requesting additional copies of this document from

Scientific Document Distribution Office (SDDO)
AECL
Chalk River, Ontario
Canada K0J 1J0

Fax: (613) 584-1745 Tel.: (613) 584-3311
ext. 4623

Price: B

Pour identifier les rapports individuels faisant partie de cette série, nous avons affecté un numéro AECL- à chacun d'eux. Veuillez indiquer le numéro AECL- lorsque vous demandez d'autres exemplaires de ce rapport au

Service de Distribution des documents officiels (SDDO)
EACL
Chalk River (Ontario)
Canada K0J 1J0

Fax: (613) 584-1745 Tél.: (613) 584-3311
poste 4623

Prix: B